

An Investigation of Reynolds Number Effect on the Aerodynamics of Bluff Body with Sharp Edges

A. Bakkhoshnevis

Department of Mechanical Engineering,
Hakim Sabzevari University
E-mail: Khosh1966@yahoo.com

A. R. Mamouri*

Department of Mechanical Engineering,
Eshragh Institute of Higher Education
E-mail: amirelmir3000@yahoo.com,
*Corresponding author

F. Mir

Department of Mechanical Engineering,
Hakim Sabzevari University
E-mail: Farzadmeer@yahoo.com

Received: 25 February 2015, Revised: 30 April 2015, Accepted: 4 May 2015

Abstract: In general, the aerodynamic stability of long span bridges is evaluated based on the results of wind tunnel tests in the low Reynolds number region, because in almost all wind tunnel tests, it is impracticable to satisfy Reynolds number similitude. Therefore, in order to correctly evaluate conventional wind tunnel test results, Reynolds number effects on the aerodynamic force coefficients acting on bridge decks must be carefully investigated. This paper investigate the Reynolds number effect on the aerodynamics of bridge deck section measured in the wide Reynolds number region from 7×10^3 to 6.1×10^4 based on the dimension of deck height in smooth flow. For the simulation of fluid flow, open-circuit and blowing wind tunnel was used for which the maximum nominal turbulence was 0.1%. The results show that increasing Reynolds number has less effect on the drag coefficient and Strouhal number and parameters in downstream of the model. In other words, variation of drag coefficient and Strouhal number is very small in Reynolds numbers over 20000. Increasing Reynolds number would not be followed with an outstanding change of the velocity defect while it results in reduction of half width with no effect on its growth rate.

Keywords: Bridge Deck, Drag Coefficient, Reynolds Number, Strouhal Number

Reference: Khoshnevis, A. B., Mamouri, A. R., Mir, F., "An investigation of Reynolds number effect on the aerodynamics of bluff body with sharp edges", Int J of Advanced Design and Manufacturing Technology, Vol. 8/ No. 3, 2015, pp. 25-32.

Biographical notes: **A. B. Khoshnevis** is an associate professor of Mechanical Engineering at Hakim Sabzevari University, Sabzevar, Iran. He received his PhD from Indian Institute of Technology of Madras Chennai (2000), India, Master of Technology from Indian Institute of Technology of Madras Chennai (1995), and BSc from Ferdowsi University of Mashhad, Iran (1990), all in mechanical engineering. His scientific interests includes experimental aerodynamic. **A. R. Mamouri** is PhD student at the Faculty of Engineering of Hakim Sabzevari University, Sabzevar, Iran. **F. Mir** received his MSc from Hakim Sabzevari University in 2013.

1 INTRODUCTION

The aerodynamic stability of a prototype is evaluated from either wind tunnel test results or the results of numerical methods using aerodynamic coefficients of a two-dimensional model. However, with either method, the Reynolds number for the wind tunnel tests is two or three orders of magnitude smaller than the Reynolds number for the prototype. Therefore, investigating the influence of the Reynolds number on the aerodynamic forces acting on the bridge section models is important for wind-resistant design.

Many research projects into Reynolds number effects and aerodynamic stability have been carried out. There is an example of research carried out by Barre and Barnard [1] using a 1:10 scale model at a Reynolds number up to 1.7×10^6 . Also, the steady aerodynamic force coefficients and Strouhal number were measured by Schewe and Larsen [2] at a Reynolds number up to 4×10^6 .

The objective of this research is to investigate the Reynolds number effect on the aerodynamics of bridge deck section measured in the wide Reynolds number region from 7×10^3 to 6.1×10^4 based on the dimension of deck height in smooth flow. The Reynolds number can be defined as the ratio of the fluid inertia force to the fluid viscous force [3]:

$$Re = \frac{UD}{\nu} \quad (1)$$

Where U is the wind speed; D the deck height; and ν is the kinematic viscosity.

2 TEST CONDITION

In this section, first, a review of some cases where Reynolds number effects have been depicted for bridge decks is presented. Observations are based on full-scale measurements compared to wind-tunnel tests. The Storebælt East Bridge in Denmark is a remarkable structure with a 6784 m long closed-box girder steel deck. The center portion of the structure is a 2716 m long suspension bridge with a streamlined deck, having a width B to depth D ratio of approximately 7.7 (see Fig. 1). The suspension bridge is flanked by two approach bridges, 1538 and 2530 m long. The steel girder of the approach bridges is also a closed box but is bluffer than the suspension bridge deck, with a B/D of 3.7 (Fig. 1).

The Ikara Bridge in Japan was also the object of several model scale experiments at 1:20, 1:30 and 1:121 scale. Full-scale measurements during construction were also conducted, including surface pressure measurements provided an evaluation of the Strouhal number [4]. The

bridge has a closed-box girder deck, with a B/D of 5.5 and is relatively streamlined (see Fig. 2). Kubo et al. [4] addressed the issue of Reynolds number in their study of the bridge and concluded that for this type of deck cross-section, a minimum Reynolds number of $Re=110000$ (based on the deck width, B) should be respected in model scale experiments. This minimum was defined by inspection of the relationship between Strouhal number and Reynolds number, a Strouhal number of 0.16 have been measured at a Reynolds number of 20,000 compared to $St=0.20$ in full-scale. However, for the deck cross-section of the Approach Bridges of the Storebælt East Bridge, a minimum Re of 500000 can be defined from Schewe and Larsen's study [5].

Nanjing 4th bridge of Yangtze river in Jiangsu Province of southeast of China is a three span suspension bridge with main span 1418m. The original design of bridge deck is a trapezoidal steel box girder with overall width of 37.7m and a height of 3.4m (see Fig. 3). For the simulation of fluid flow, open-circuit and blowing wind tunnel was used for which the maximum nominal turbulence and velocity were 0.1% and 30m/s, respectively. In order to assess the flow, the temperature-constant hot-wire anemometer was utilized.

The main properties of the wind tunnel and the model used in this research are given in Table 1. Since the flow is 2-dimensional and the fact that the length of the model has no effect in flow results, the length is set equal to the width of the test section which is 40cm. Schematic of the wind tunnel and the section model mounted in the wind tunnels are shown in figures 5, and 6, respectively.

3 VALIDATION

To ensure correct operation of the tunnel and creating a suitable model in the section tunnel, calibration tests are essential to be done. For this, firstly free flow was measured in the test section using hot-wire sensor to ensure that the flow profile is uniform. The average speed chart for the 10 and 20 meters per second speed is shown in Fig. 7. Another experiment was conducted to measure the free stream turbulence intensity at different speeds of the tunnel (Fig. 8). According to the disturbance graphs of the wind tunnel test section, the intensity of turbulence is about 0.06%. Following the survey accuracy and performance of the wind tunnel and hot-wire anemometer, a sample of data were obtained and compared with the results of work by other researchers. Since we could not find any similar investigation on these models in the past researches, a cubic cylinder was used. Profiles of the mean velocity for the longitudinal component of velocity (u) for a

sample cubic cylinder with fineness ratio of B/D = 1 and Reynolds number of 8600 in two different stations is presented in Fig. 9. As it is shown in the figure, there are good agreement between current results and the findings of khoshnevis et al. [6], Shadaram et al. [7] and Saha et al. [8] where all the experiments are conducted with similar Reynolds number.

The Reynolds number is thus a similitude parameter that generally needs to be respected for a model-scale laboratory experiment involving fluid to be representative of full-scale conditions. Therefore, the main idea about the bluff bodies with sharp edges such as bridge decks and towers, buildings and many structural members is that the Reynolds numbers above 10000 have negligible effect on aerodynamic characteristics, as pointed by Larose and D'Auteuil [9]. The results of this research verify this too.

4 WAKE-SURVEY EQUATIONS

When a solid body is dispersed in liquid with movement with respect to each other, a force is applied from liquid to the floating body. The applied force from liquid to the moving body is originated from the dynamic interaction between liquid and body while forces such as gravity and bouncy forces have no effect. This force could be divided into two components; one along the flow and another perpendicular to the flow known as drag and lift, respectively.

Pressure gradient in front and back of the body as well as shear stresses have contribution in creation of this force. The resultant pressure gradient between high-pressure zone in front of the body and low-pressure zone at the back causes an intense drag force known as pressure drag. This force along with shear stresses being on the surface of the body along the flow direction makes the total drag force.

Relative contribution and pressure drags in total force depend on the body shape, amplitude of surface up and down and also thickness of the body. If the thickness is negligible, i.e., the body is approximated with a flat plate, all the drag force applied on the body could be assumed as frictional drag. Considering this point, in the current sample, flow lines move in parallel form and without separation from the surface with no pressure gradient in front and back of the body.

With regard to experimental approach for computing drag coefficient, Chao and Van Dam [10] have conducted much research in order to investigate the effects of turbulence intensity on drag force measurement. Van dam [11] obtained an equation for calculating the drag coefficient in which expressions respectively, where Reynolds stresses and viscose are neglected. The equation is presented as follows:

$$C_d = \int \left(\frac{P_{sa} - P_{sw}}{q_\infty} \right) d\left(\frac{z}{c}\right) + 2 \int \frac{\bar{u}}{U_\infty} \left(1 - \frac{\bar{u}}{U_\infty} \right) d\left(\frac{z}{c}\right) - 2 \int \frac{\bar{u}'^2}{U_\infty^2} d\left(\frac{z}{c}\right) \quad (2)$$

$$q_\infty = \frac{1}{2} \rho (\bar{u}^2 + \bar{v}^2 + \bar{w}^2) \quad (3)$$

As is clear, Eq. 2 includes the following three parts: Pressure:

$$\int \left(\frac{P_{sa} - P_{sw}}{q_\infty} \right) d\left(\frac{z}{c}\right) \quad (4)$$

Momentum:

$$2 \int \frac{\bar{u}}{U_\infty} \left(1 - \frac{\bar{u}}{U_\infty} \right) d\left(\frac{z}{c}\right) \quad (5)$$

Reynolds stress:

$$2 \int \frac{\bar{u}'^2}{U_\infty^2} d\left(\frac{z}{c}\right) \quad (6)$$

However, according to Goldstein analysis [12]:

$$P_{sa} = P_{sw} + \bar{q}' \quad (7)$$

$$\bar{q}' = \frac{1}{2} \rho (\bar{u}'^2 + \bar{v}'^2 + \bar{w}'^2) \quad (8)$$

Finally, we have:

$$C_d = 2 \int \sqrt{\frac{\bar{q}}{q_\infty}} \left(1 - \sqrt{\frac{\bar{q}}{q_\infty}} \right) d\left(\frac{z}{c}\right) + \frac{1}{3} \int \left(\frac{\bar{u}'^2 + \bar{v}'^2 + \bar{w}'^2}{U_\infty^2} \right) d\left(\frac{z}{c}\right) \quad (9)$$

Using Eq. 9, it is possible to obtain the drag coefficient with the wake-survey method.

5 CROSS-WIND VIBRATIONS INDUCED BY VORTEX SHEDDING

Vortex-induced vibrations occur when vortices are shed alternately from opposite sides of the structure. This gives rise to a fluctuating load perpendicular to the wind direction (see Fig.10). When a vortex is formed on one side of the structure, the wind speed is increased on the other side and according to the Bernoulli's theory (Eq. 10), these results in reduced pressure. Thus, the structure is subjected to a lateral force away from the side where a vortex is formed. As the vortices are shed alternately first from one side then the other, a

harmonically varying lateral load with the same frequency as the frequency of the vortex shedding is formed. In most practical situations the idealized flow pattern described with one vortex shedding frequency is modified due to air turbulence [13].

$$P + \frac{1}{2}\rho U^2 = \text{Constant (along a streamline)} \quad (10)$$

In most sample configurations, a stable street of staggered vortices forms behind the structures as in Fig.10. The along-wind velocity, U_1 , of the vortices is approximately $0.85U$, where U is the wind velocity in the undisturbed field. This vortex street has been analyzed by the Von Karman, and is called a von Karman vortex street.

For a non-vibrating structure the distance l_v between vortices rotating in the same direction must be proportional to the structure width, d , perpendicular to the direction of the wind, since d is the only relevant length. The time between the vortices equals distance l_v divided by velocity U_1 of the vortices. This means that frequency n_s of the lateral load caused by vortex shedding is U_1/l_v , which is proportional to U/d . The factor of proportionality is called the Strouhal number St , so:

$$St = \frac{fD}{U} \quad (11)$$

Where

St: Strouhal number (—)

f: Vortex shedding frequency (1/s)

D: Deck height (m)

U: Wind speed (m/s)

6 EVOLUTION OF WAKE VELOCITY FIELD

The flow field in the wake behind the bridge model is traversed with a hot wire probe. Sampling the time series of the hot wire exposed to highly turbulent flow in the model wake, a signal of high frequency is recorded. The signal is evaluated regarding the mean velocity deficit $\frac{u}{U}(-)$ and the turbulence intensity $\frac{u'}{U}(\%)$ in the wake [14]. The measurements are presented for four axial measurements stations $X/B = 0.01, 0.5, 1, 2$.

The velocity defect is presented as follows:

$$W_o = \frac{(\frac{u}{U})_{max} - (\frac{u}{U})_{min}}{(\frac{u}{U})_{max}} \quad (12)$$

Half width ($b_{1/2}$) is representative of half of wake width (Fig. 11).

7 RESULTS AND DISCUSSION

A shallow deck combined with a streamlined aerodynamic geometry, which results in small drag force, is one of the design criteria for modern long-span cable-supported bridge decks. As a consequence, the size of the supporting cables and of the towers can be reduced, resulting in lighter structures which in turn reduces the construction cost. Results in this study show that increasing Reynolds number has less impact on the drag coefficient and Strouhal number. In other words, variation of drag coefficient and Strouhal number is small in Reynolds numbers over 20000 (Fig. 12).

The Reynolds number is thus a similitude parameter that generally needs to be respected for a model-scale laboratory experiment involving fluid to be representative of full-scale conditions. For a bluff body with sharp edges, it is believed that the onset of the flow separation is defined by the location of the edges, and flow re-attachment may or may not occur but if it does, it might not be affected by Reynolds number. The Reynolds number similitude parameter is thus generally relaxed in wind engineering studies where the effects of wind on buildings and bridges are investigated on models at Re one or two orders of magnitude lower than in full scale [9].

Figure 13 shows the plot of velocity defect at different positions as well as various Reynolds numbers. Variation of Reynolds number and location of station causes difference in value of the parameter corresponding to the velocity defect. As it goes toward downstream, velocity defect reduces while variation amplitude reaches its minimum value at final stations. Also, increasing Reynolds number would not be followed with an outstanding change at the value of velocity defect.

Unlike the velocity defect, value of half width is increasing while moving downstream which is due to widening of the wake whereas with increasing Reynolds number, it still reduces sharply. Of course, Reynolds number has no effect in rate growth of half width. Moving toward downstream, turbulence intensity reduces which is due to vortices lessening far from the model. However, it is observed that increase of Reynolds number ($Re > 32000$) will not bring about a change in the maximum value of turbulence intensity (Fig. 14).

8 FIGURES AND TABLES

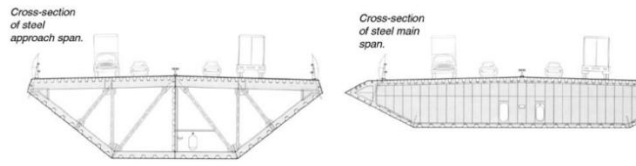


Fig. 1 Deck cross-sections for the Storebælt East Bridge, Approach Bridge (left), Suspension Bridge (right)

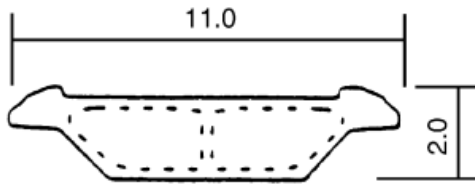


Fig. 2 Deck cross-section for the Ikara Bridge, after Kubo et al. [4] (dimensions: m)

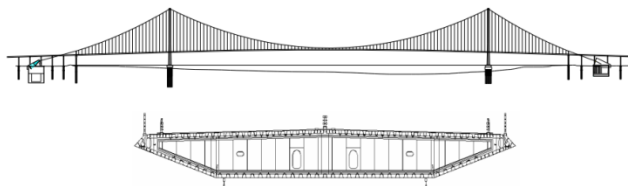


Fig. 3 Outline of Nanjing Yangtze 4th Bridge

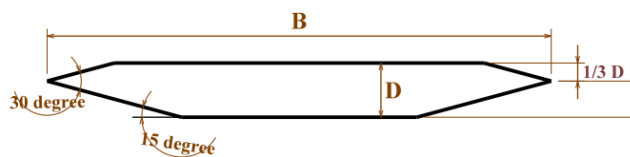


Fig.4 Basic box girder cross section

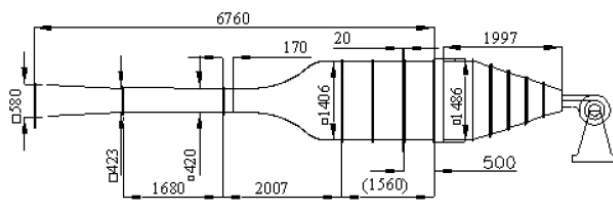


Fig. 5 Schematic of a wind tunnel (Unit: mm)

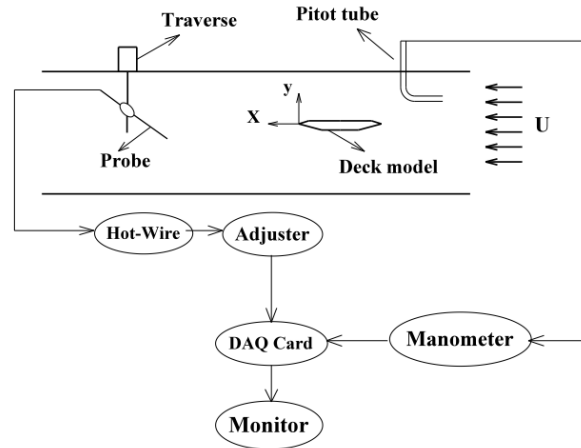


Fig. 6 Scale model mounted in the wind tunnel

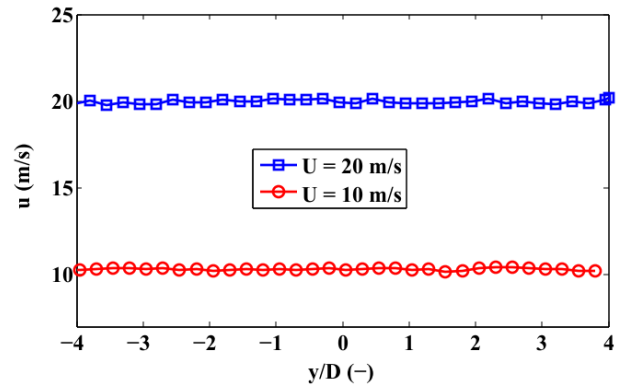


Fig. 7 Variation of average speed in the wind tunnel for input speeds of 10 and 20 m/s

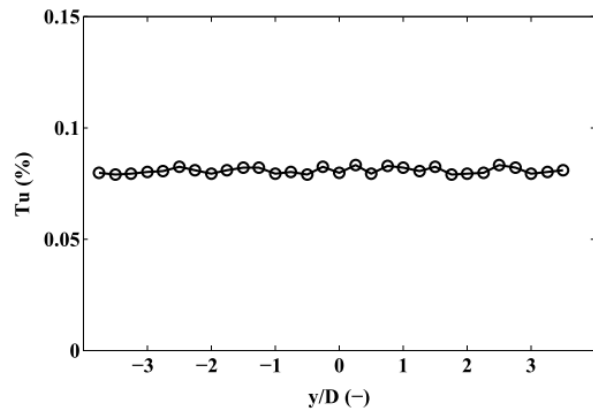
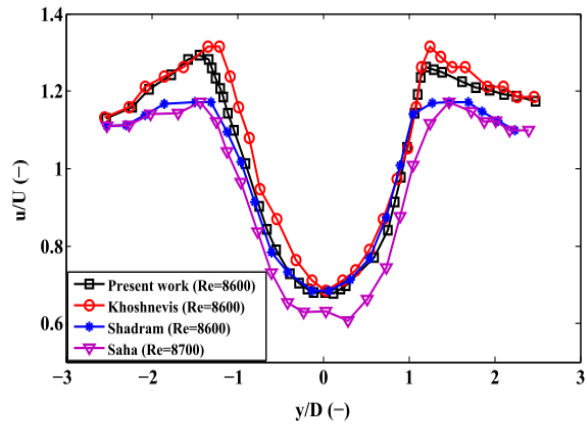
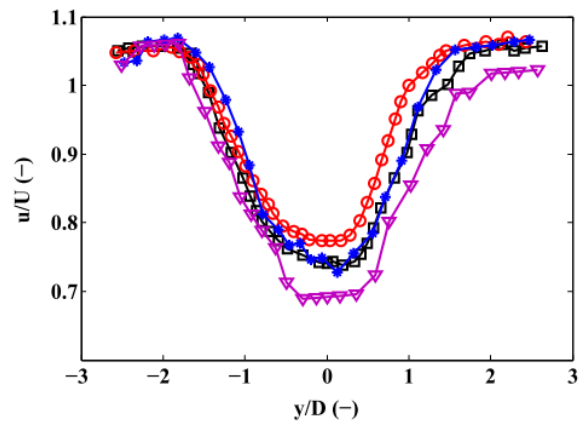


Fig. 8 The variation of turbulence intensity in the wind tunnel at a speed of 10 m/s



a) $X/B = 1$



b) $X/B = 2$

Fig. 9 Profile of mean velocity for square cylinder in two different stations

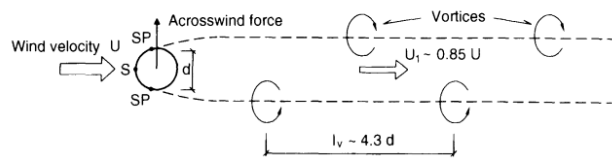


Fig. 10 Principal sketch of Vortex Street behind a cylinder

S is the point of stagnation, i.e. the foremost point of the cylindrical cross section. SP is the point of separation where the vortices separate from the structure.

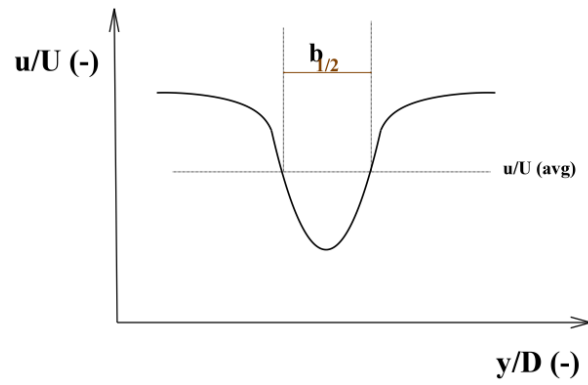


Fig. 11 Parameter of half width in the wake

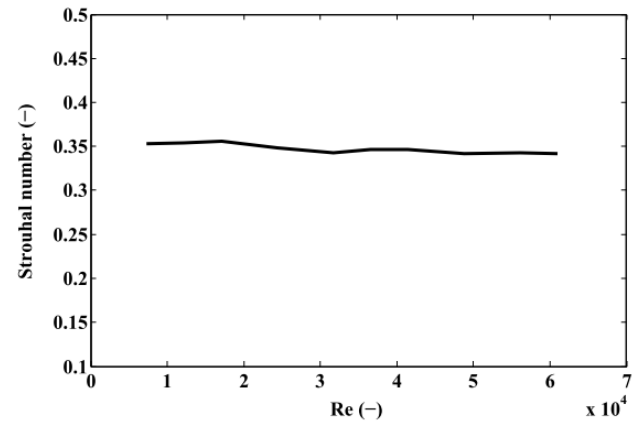
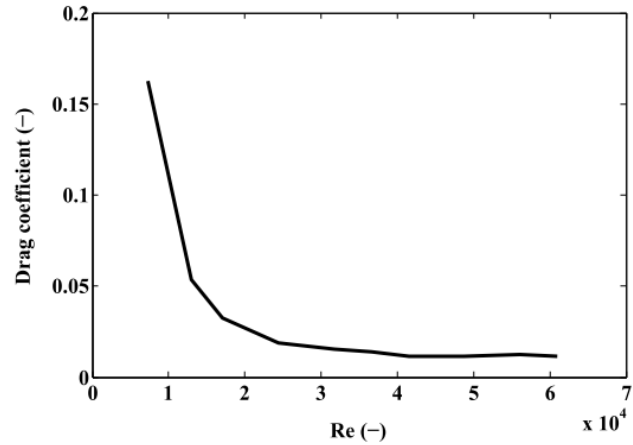


Fig. 12 Variations of drag coefficient and Strouhal number

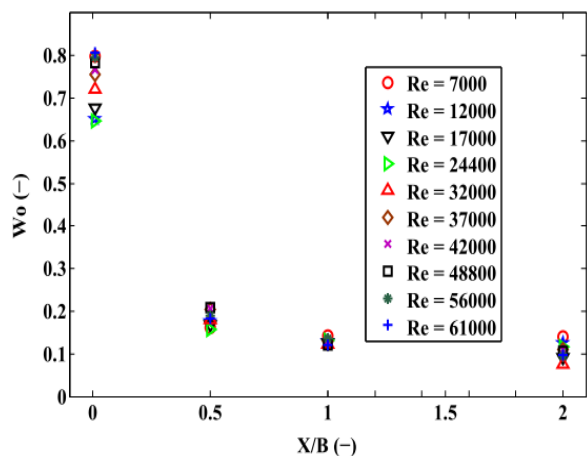


Fig. 13 Variation of Velocity defect and half width of wake

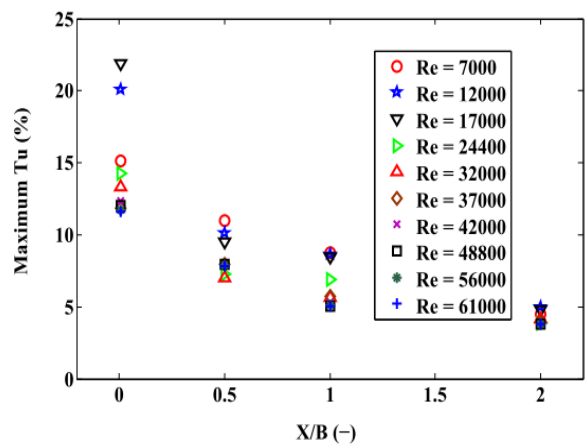
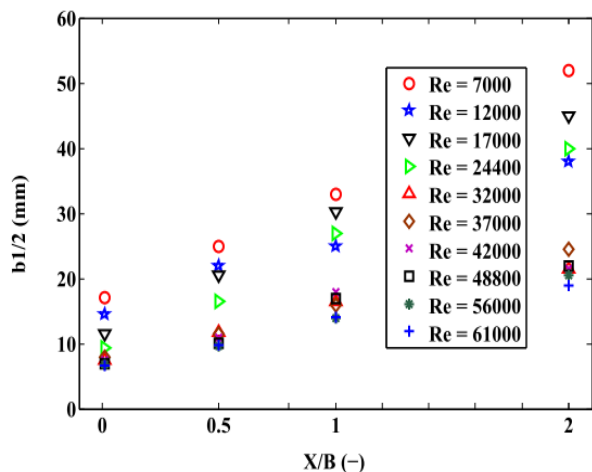


Fig. 14 Maximum turbulence intensity in downstream of model

Table 1 The main properties of the wind tunnel and the model

Test section wind tunnel		
Width, cm	Height (H), cm	Wind speed, m/s
40	40	2.86-25
Deck model		
Width (B), cm	Height (D), cm	Fineness ratio (B/D)
28	3	9.33
Reynolds number (Re_D)		
7000-61000		
Blockage ratio (D/H)		
0.075		

9 CONCLUSION

This paper investigated the effects of Reynolds number on the aerodynamic of bridge deck section measured from the wake flow. The results showed that increasing Reynolds number has less effect on the drag coefficient and Strouhal number. In other words, variation of drag coefficient and Strouhal number is very small in Reynolds numbers over 20000. Also, Increasing Reynolds number would not be followed with an outstanding change at the value of velocity defect and maximum turbulence intensity while it results in reduction of half width with no effect on its growth rate. Moving toward downstream, turbulence intensity reduces which is due to the vortices lessening far from the model. However, it is observed that increase of Reynolds number ($Re > 32000$) will not bring about a change in the maximum value of turbulence intensity.

10 NOMENCLATURE

- X: stream wise coordinate measured from the rear surface of the trailer.
- y: vertical coordinate measured from the down surface of the trailer
- D: height of deck model
- B: width of deck model
- H: height of the test section
- U: free stream velocity
- u: stream wise component of velocity
- Tu: Turbulence intensity percent

REFERENCES

- [1] Barre, C., Barnard, G., “High Reynolds number simulation techniques and their application to shaped structures model test”, Proceedings of First IAWE European and African Regional Conference, Guernsey, UK, 1993, pp. 83-93.
- [2] Schewe, G., Larsen, A., “Reynolds number effects in the flow around a bluff bridge deck cross section”, Proceedings of Second IAWE European and African Regional Conference, Genova, Italy, 1997.
- [3] Tanaka, H., “Similitude and modelling in bridge aerodynamics”, Proceedings of the First International Symposium on Aerodynamics of Large Bridges, Copenhagen, Denmark, 1992, pp. 83-94.
- [4] Kubo, Y., Nogami, C., Yamaguchi, E., Kato, K., Niihara, K. and Hayashida, Y., “Study on Reynolds number effect of a cable-stayed bridge girder”, in: A. Larsen, G.L. Larose, F.M. Livesey (Eds.), Wind Engineering into the 21st Century, Vol. 2, Balkema, Rotterdam, 1999, pp. 935-940.
- [5] Schewe, G., Larsen, A., “Reynolds number effects in the flow around a bluff bridge deck cross section”, J. Wind Eng. Ind. Aerodyn., Vol. 74–76, 1998, pp. 829-838.
- [6] Khoshnevis, A. B., Barzanoi, V., and Foroozesh, F., “Experimental Investigation of the Aerodynamic of a Car Model”, International Journal of Advanced Design and Manufacturing Technology, Vol. 6. No. 1, 2013.
- [7] Shadaram, A., Azimi-Fard, M., and Rostamy, N., “Experimental study of flow characteristics in wakes adjacent to squared section cylinders”, Mechanics and Aerospace Publication, 2006, pp. 3.
- [8] Saha, A. K., Muralidhar, K., and Biswas, G., “Experimental study of flow past square cylinder at high Reynolds numbers”, Experiments in Fluids, 2000, pp. 553.
- [9] Larose, G. L., Auteuil, A. D., “On the Reynolds number sensitivity of the aerodynamics of bluff bodies with sharp edges”, J. of Wind Eng. And Industrial Aerodynamics, Vol. 94, 2006, pp. 365-376.
- [10] Chao, D., Van Dam, C. P., “Airfoil Drag Prediction and Decomposition”, J. of Aircraft., Vol. 36, No. 4, 1999, pp. 675-681.
- [11] Van Dam, C. P., “Recent Experience with Different Methods of Drag Prediction”, Progress in Aerospace Science, Vol. 35, 1999, pp. 751-798.
- [12] Goldstein, S., “A Note on the Measurement of Total Head and Static Pressure on a Turbulent Stream”, Proceedings of the Royal Society of London, Series A, Vol. 155, 1936, pp. 570-575.
- [13] Dyrbye, C., Ole Hansen, S., “Wind Loads on Structures”, 1997. Originally published in Danish as Vindlast på * bærende konstruktioner © 1989 Statens Byggeforskningsinstitut.
- [14] Finn, E., Jørgensen, “How to measure turbulence with hot-wire anemometers”, Publication no.: 9040U6151. Date 2002-02-01. Dantec Dynamics A/S, P.O. Box 121, Tonsbakken 16-18, DK-2740 Skovlunde, Denmark, 2002.